A new methodology for the mechanical behavior analysis of polyvinyl chloride and recycled polyethylene terephthalate foams: Finite element model updating using mechanical field measurements

Joulia Salloum, Romain Léger, Hussein Chebbo, Loïc Daridon, Patrick Ienny

A new methodology for the mechanical behavior analysis of PVC and recycled PET foams: Finite element model updating using mechanical field measurements

Joulia Salloum[1], Romain Léger[1], Hussein Chebbo[1], Loïc Daridon[2], Patrick Ienny[1]

[1] LMGC, IMT Mines Ales, Université de Montpellier, CNRS, Ales, France

[2] LMGC, Université de Montpellier, CNRS, Montpellier, France

Keywords: FEMU method; PVC foam; recycled PET foam; Sandwich composite materials; intrinsic properties.

Abstract

This paper aims to characterize the intrinsic mechanical behavior of an eco-friendly foam core used in sandwich materials dedicated to the maritime sector. A thorough understanding of intrinsic properties is essential for accurate dimensional structure characterization. The model setup is based on the choice of materials that meet the criteria of sustainable development, mechanical performance, and durability to promote ecological practices in the nautical industry. Experimental tests, instrumented by a digital image correlation technique, were carried out on two types of foams: polyvinyl chloride (PVC), which is the reference foam traditionally used in marine applications, and recycled polyethylene terephthalate (rPET), the substitute foam. The sample sizes recommended by compression test standards often lead to complex stress states that do not allow direct determination of the foam's intrinsic mechanical properties. Therefore, a finite element model updating method was required to identify the anisotropic elastic behavior of these two types of foams.

1. Introduction

Like most materials used for structures, sandwich materials are no exception to the current trend to replace traditional components with more eco-friendly counterparts. The difficulty in

this substitution often comes from the inferior mechanical properties of the substitute materials, which calls into question the dimensioning of structures. The research project herein aims to define simple rules for designing sandwich materials based on eco-friendly materials for applications in the nautical field. The design is therefore based on the choice of environmentally friendly materials that can offer similar mechanical properties compared with traditional sandwich materials. In this paper, the core material is the one that will be studied. As such, polymer foams are often used as the core material of the sandwich structure. Commercially available polymeric foams for structural applications are polyvinyl chloride (PVC) foams, polyurethane (PU) foams, and polyethylene terephthalate (PET) foams. Polymer foams belong to the class known as solid foams, which are versatile materials (1). They are also called cellular materials, where their porous solid structure comprises pores or cells filled with a gaseous phase (2). Polymeric foams, being thermoplastic materials, can be manufactured by different manufacturing processes: injection foaming, extrusion foaming, and gelation (3). All these foam manufacturing processes are carried out using the same steps to create their cellular structure. Generally, the compressive strength of polymeric foams is higher than their tensile strength (4)(5)(6)(7) because their cellular structure is better suited to withstand compressive rather than tensile forces. Accordingly, in most cases, polymeric foams are mainly loaded in compression. In the case of this loading mode, the homogeneous equivalent macroscopic mechanical behavior can be described by three main stages (8): an initial linear elastic domain characterized by an equivalent elastic stiffness modulus and an equivalent transverse contraction coefficient, a plateau domain that can be described phenomenologically by yield stress and strain hardening slope, and finally, a densification domain, where the material exhibits volume type behavior. Francisco et al. (9) studied the mechanical behavior of closed-cell PVC foam under compressive loading. They observed that heterogeneity and anisotropy greatly influence the mechanical response of this material

studied under different directions of compressive loading. For example, the yield stress and the compressive modulus are higher in the thickness or longitudinal direction of the foam (out-of-plane) than that in the transverse direction (in-plane). Luong et al. (10) studied the compressive properties of closed-cell PVC foam for different densities. As a result of their work, the density of the foam influences the force values at the peak and the plateau after the elastic part: foams with higher density offer better mechanical properties. Viana and Carlsson (11) concluded that cross-linked PVC foams with different densities have an almost isotropic behavior. This result was based on a study conducted by the authors to determine the mechanical properties (stress-strain response) and the fracture behavior of these materials. The study mainly consisted of tensile tests and a comparison of the stiffness modulus obtained along the two longitudinal and transverse directions. Volnei Tita et al. (12) studied the anisotropic mechanical behavior of polyvinyl chloride (PVC) foams with a density of 60 kg/m^3 (Divinycell H60). This study discussed the challenges of assessing the mechanical properties of foams due to their anisotropy and heterogeneity (13),(14). It was shown through experimental analysis how the foam's microstructure affects its mechanical behavior using both compression and tensile in two material directions, longitudinal and transverse. It was shown that the studied foam was transversely isotropic. However, the mechanical properties can vary significantly depending on the loading direction and the testing method, whereas the material's microstructure also affects the phenomenological response, failure mechanisms, and hardening curves. Many research articles have discussed collecting or estimating material properties for cellular materials, particularly for compression loading, using standardized methods (11), (15). Much work has been done to study the mechanical behavior of polymeric foams, either on their experimental or numerical mechanical characteristics, such as the work of (5),(7),(16), (17), (18), (19). However, none of these studies have led to the determination of the intrinsic parameters of the foams. Standardized tests concerning foams, mainly

sandwiches, do not make it possible to directly identify intrinsic properties due to the geometry of the samples. These tests are most often conducted under multiaxial stress conditions due to the thin thickness of the foams, and the boundary conditions used in these tests are often not designed to ensure being in a homogeneous stress state. As a result, the data used by ship designers is approximative and, therefore, leads to oversized structures. As a viable solution, interpreting these tests requires numerical finite element modeling. This paper aims to determine, by a finite element model updating (FEMU) method (20)(21)(22), the intrinsic elastic parameters of two types of foams: a regular PVC and a rPET, both having a density of 80 kg/m^3, in order to study the potential substitution of the former with the latter, thus providing a more environmentally friendly and sustainable alternative.

2. Materials and methods

2.1. PVC and recycled PET foams

Two types of foams, a polyvinyl chloride (PVC) foam of commercial name "AIREX C70" and a recycled polyethylene terephthalate (rPET) foam of commercial name "ArmaForm Core" were studied in this paper. The PVC foam represents the reference material to be substituted by the rPET foam. Both are closed-cell foams with the same 80 kg/m^3 density. A summary of their different characteristics, taken from their technical sheets, is given in Table 1. These two foams are in the form of large rectangular plates having a thickness of 15 mm. The large sheets of rigid closed-cell foams were cut using a mechanical saw to prepare the specimens.

Table 1: PVC and rPET foams' mechanical characteristics taken from supplier data sheets.

		Compression properties		**Shear properties**	
Foam	Density [kg/m^3]	Standardized test	Compressive Modulus [MPa]	Standardized test	Shear Modulus [MPa]
PVC	80	DIN 53421 (superseded by ISO 844:2021) (23)	Average: 104 Minimum: 80	ASTM C393 (24)	Average: 30 Minimum: 24
rPET	80	ISO 844:2021 (23)	57	ISO 1922:2018 (25)	16

2.2. Compression tests on foams

Based on ISO 844:2021 standard, the compression tests were performed using a MTS Criterion C45.105 machine equipped with a 1 kN load cell and instrumented by two CCD cameras to get the 2D full-field deformation measurements of the front and lateral faces of each specimen by digital image correlation technique. The cameras (SVS-Vistek svs2150XTLGEC model) equipped with 55 mm / F2.8 telecentric lens (Computar REC-M55 model) were positioned in front of these faces to record images of resolution 1920 x 1080 (pixel size 75 µm) at a sampling rate of 5 fps. The compression was carried out by applying a displacement on the top face of the specimen. The crosshead speed was set for each specimen to obtain a strain rate of 1.1×10^{-2} s^{-1}. The evaluation of the in-plane strain tensors on each observed face of the sample by DIC technique was performed with a home-developed software called 'CinEMA' (22) which enabled the calculation of the different apparent elastic modulus and transverse contraction coefficients. The evaluation of the strain tensor at the sample surface is based on local least-squares adjustment, using a linear fit of the displacement field around the considered point contained in the suitable gauge length. Two gauge lengths have been defined depending on whether an average deformation (global approach) or a deformation profile (local approach) is measured over the entire surface of the sample. While the deformation profiles, analyzed by DIC, are associated with a 2 mm (30 pixels) gauge length, the stress-strain curves are associated with a 14 mm (187 pixels) gauge length. The nominal stress is defined as the ratio between the uniaxial force recorded by the test equipment and the initial cross-sectional area of the sample. Sample dimensions are essential in such a study. The foam sheets used in this paper have a thickness of 15 mm, so to conduct a uniaxial compression test, specimen dimensions should have had a width less than or equal to half of its thickness, i.e., 7.5 mm. These tests are not feasible given the complexity

of conducting compression tests on such small specimens and the size of the representative elementary volume (REV) of the morphology of these foams. Consequently, compression tests were conducted on larger samples, as ultimately recommended in the standards. However, these do not correspond to simple uniaxial compression tests but to triaxial compressions tests that do not directly lead to determining the intrinsic properties of the foams studied herein. In addition, it is essential to consider the representativity of the volume occupied relative to the pore size. If the specimen is too small compared to the pore size in the foam, it may result in a large dispersion in the compression measurements. Therefore, scanning electron microscopy (SEM) was used to verify the pore size in both foams. It helped to ensure that the specimen dimensions were appropriate for the pore size, and accordingly, the compression tests conducted would represent the foam's properties. SEM visualizations at the same magnification along the thickness direction $\overrightarrow{e_3}$ of PVC and rPET foams are represented in Figures 1 (i) and (ii).

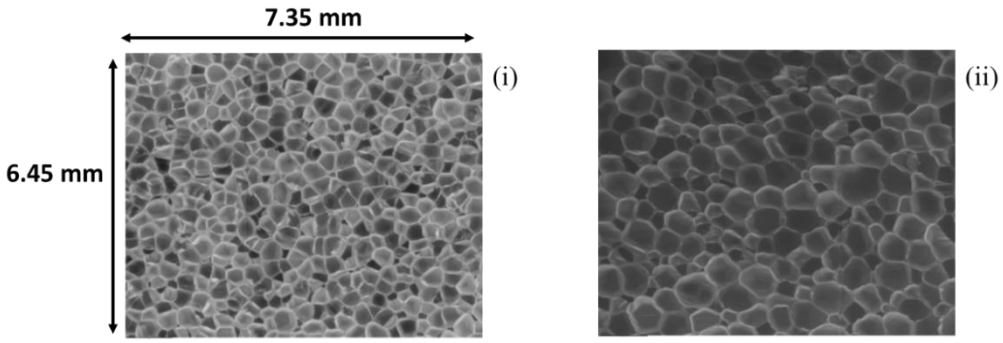

Figure 1: SEM results - (i) PVC foam, (ii) rPET foam.

The pore size of the rPET foam was observed to be larger than that of PVC. Indeed, for both foams, the average area of the pores was calculated using ImageJ software, and the results are displayed in Figure 2 along the three normal directions, $\overrightarrow{e_1}$, $\overrightarrow{e_2}$, and $\overrightarrow{e_3}$, representing length, width, and thickness or height of the foam, respectively. The dimensions of the chosen specimens for compression tests were deemed sufficient compared to the pores' size, thus ensuring that the experimental test results would be representative and accurate. As an

additional observation, the pore size isotropy observed for PVC does not seem to be obtained for rPET. Based on these explanations, multiaxial compression tests were carried out on 15x15x15 mm^3 cubic specimens along two directions: the $\overrightarrow{e_3}$ axis (in the thickness) and the $\overrightarrow{e_2}$ axis, as shown in Figure 3 (i). The correspondent apparent stiffness modulus and the apparent transverse contraction coefficients are obtained in both directions.

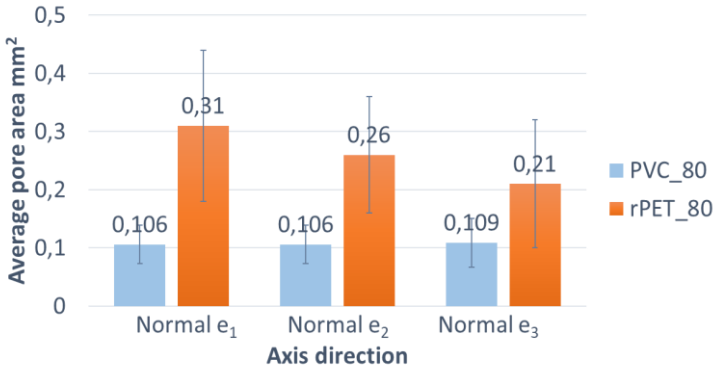

Figure 2: SEM results - Average pore area for PVC and rPET foams.

These tests confirm the transverse isotropy assumption discussed in the literature (12), as they cannot determine the foam's intrinsic elastic properties. In addition, to complete the triaxial stress conditions, the transverse dimension of 15 mm was extended to 30 mm and then 60 mm. However, a uniaxial compression test can still be performed on the foam along the $\overrightarrow{e_2}$ or $\overrightarrow{e_1}$ axis direction by sectioning the specimen to have a length greater than two times the width, and the thickness, respectively, thus enabling a uniaxial stress state along this direction. Accordingly, specimens of 15x40x15 mm^3 were cut to carry out uniaxial compression tests along the $\overrightarrow{e_2}$ axis direction (Figure 3 (ii)). It is worth noting that no uniaxial compression tests along the $\overrightarrow{e_1}$ axis direction were made. The rationale behind this decision will be explained later in this paper.

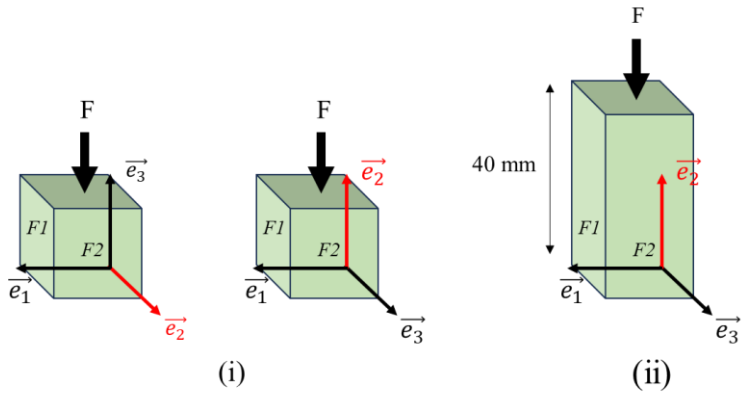

Figure 3: (i) Triaxial compression test along the $\overrightarrow{e_3}$ and $\overrightarrow{e_2}$ axis, (ii)Uniaxial compression test along the $\overrightarrow{e_2}$ axis (F1 and F2 indicates faces observed with cameras).

2.3. Shear tests on foams

Shear tests were carried out on the two types of foams based on ISO 1922:2018 standards. To be able to perform these shear tests using the MTS Criterion C45.105 machine, the samples were prepared by bonding four steel sheets, each having dimensions of 100x40x5 mm^3, with foam parts on both sides, as shown in Figure 4. A bio epoxy resin (SR InfuGreen 810 from the company Sicomin®) was used as a bonding agent. The test was conducted by applying a displacement on one side of the specimen and fixing the other. The crosshead speed was set to 10 mm/min. Images of the sample were taken during the test using the same setup as the one described in the Compression tests on foam section. The DIC technique was used to obtain the strain field and to calculate the corresponding shear modulus. Shear tests in two different planes, ($\overrightarrow{e_1}$, $\overrightarrow{e_3}$) and ($\overrightarrow{e_1}$, $\overrightarrow{e_2}$), were conducted on the two types of foam. For the tests in the ($\overrightarrow{e_1}$, $\overrightarrow{e_3}$) plane, four foam specimens measuring 40x40x15 mm^3 were prepared. In contrast, for the shear tests in the ($\overrightarrow{e_1}$, $\overrightarrow{e_2}$) plane, eight foam specimens measuring 15x40x15 mm^3 were cut due to the limitation of 15 mm in the $\overrightarrow{e_3}$ direction. Figure 4 illustrates the setup of the bonded foam parts on the steel plates.

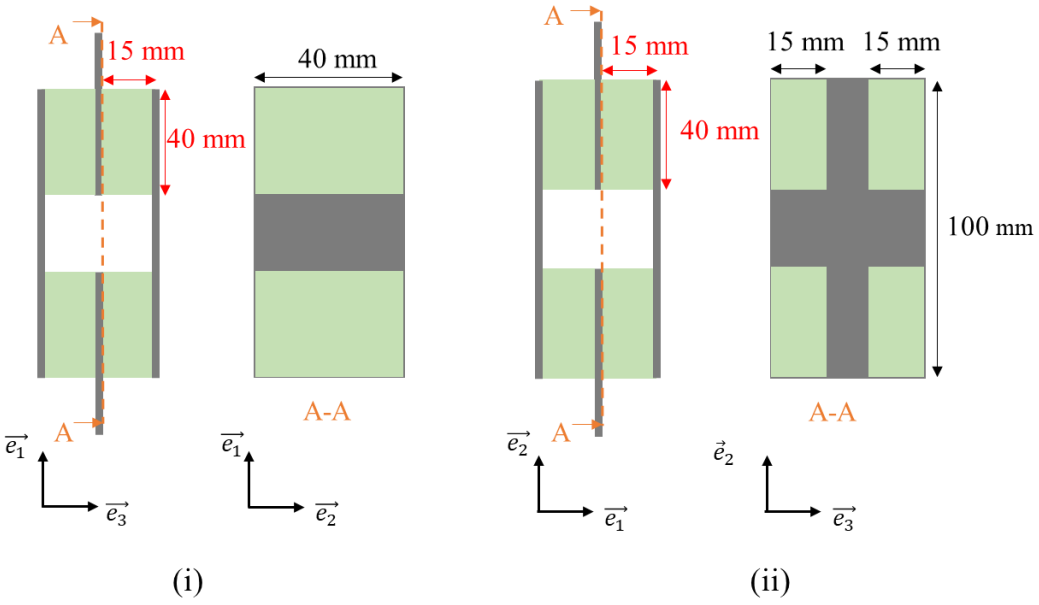

Figure 4: (i) Shear test in ($\vec{e_1}$, $\vec{e_3}$) plane, (ii) Shear test in ($\vec{e_1}$, $\vec{e_2}$) plane.

2.4. FEMU method

In the case of a sample with a width greater than its height undergoing a compression test, the stress state cannot be considered uniaxial compression. Instead, it is a multiaxial stress state, also known as a large compression test, which requires a numerical model to determine the intrinsic mechanical characteristics of the sample material. So, in this study, the FEMU method is used to identify the intrinsic elastic parameters of PVC and rPET foams based on the experimental data. This method updates the finite element model by adjusting its parameters until its resulting force response matches the experimental values. As such, the force response was used to achieve the minimization process, and the displacement values were used to define the boundary conditions. The model was created on Abaqus from a Python code with imposed different boundary conditions. A minimizing algorithm existing in Matlab called "fmincon" was used to recalibrate the model on Abaqus by comparing the calculated numerical values with the experimental measurements. Additionally, input parameters needed for this adjusting method are the specimen's dimensions, material properties (density and elastic parameters), and mesh size, while output parameters are only

the adjusted elastic parameters. Further details on this method, including boundary conditions, are presented later in the Numerical elastic model section of the article. The element type used in Abaqus® is 3 degrees of freedom (DOF) hexahedral linear element.

3. Experimental results

3.1. Reproducibility of tests

Multiple tests were carried out to obtain reproducible results precisely by following standardized protocols and using calibrated equipment to conduct the different experimental tests to ensure the findings were valid and reliable. The findings' reproducibility was confirmed by replicating the experiments ten times. The graphs displayed in Figures 5 (i) and (ii) below show an example of the reproducibility of the force-displacement curves for ten specimens (15x15x15 mm^3) for each foam (PVC and rPET) under compression loading. This result also confirms the choice of a test geometry representative of the material's morphology (REV).

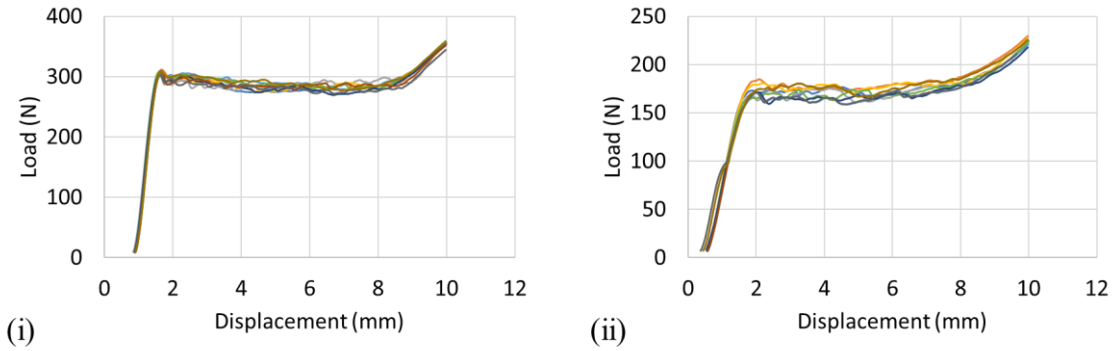

Figure 5: Force-displacement curves for 10 specimens (15x15x15 mm^3) - (i) PVC, (ii) rPET.

Although this paper primarily focuses on the elastic behavior of the foam, the yield stress is also an intrinsic quantity widely used in the design basis of components and structures. The experimental measurements of the apparent yield stress obtained are about 1.37 MPa and 0.78 MPa for PVC and rPET foams, respectively, meaning that substituting PVC with rPET would lead to an oversizing of the structure. Although the study of the collapsed part of the foam is not yet made, this observation could shed light on the differences in mechanical

behavior between the two foams. Therefore, further research is needed to fully understand the mechanical behavior properties of both foams.

3.2. Triaxial compression tests

Considering that the foams studied in this paper have a thickness of 15 mm, compression tests were conducted on different sets of specimen dimensions. Three sets were tested in the thickness direction ($\overrightarrow{e_3}$ axis): a - 15x15x15 mm^3, b - 30x30x15 mm^3, and c - 60x60x15 mm^3. Compression tests in the thickness (longitudinal) direction allow obtaining the apparent stiffness modulus E_3^*. Ten samples were tested for each set of specimen dimensions (a-b-c). Before proceeding to the analysis of the results, it is necessary to gain insight into the strain field calculations in material testing, whether a real and non-homogeneous strain field needs to be calculated or, in contrast, an averaged strain field is sufficient, i.e., "local approach" or "global approach" respectively. As such, the strain profile is plotted following compression tests on the three specimen sets (a-b-c), hence, ensuring that measurements are consistent and accurate and confirming a homogeneous strain field. An example of the different strain profiles, extracted from the elastic behavior zone, is shown in Figures 6 (i), (ii), and (iii), corresponding respectively for the specimen sets a, b, and c. Based on the obtained strain profiles for both foams, it can be demonstrated that the strain field is homogeneous. The magnification factor here is about 75 µm/pixel, and about 2 mm was removed from the borders while plotting the graphs to avoid edge effects. For the same material, the obtained apparent elastic modulus increased for each set of dimensions (a-b-c), as shown in Table 2. This modulus is obtained through linear regression in the linear elastic part of the stress-strain curve by calculating its slope. As such, the slope of the linear elastic part between the strain values of about -0.0125 and -0.001 is highlighted in Figure 7. This difference in results depending on specimens' size, coming from the stresses' multiaxial nature, confirms that the standardized compression tests do not lead to identifying the foam's intrinsic characteristics.

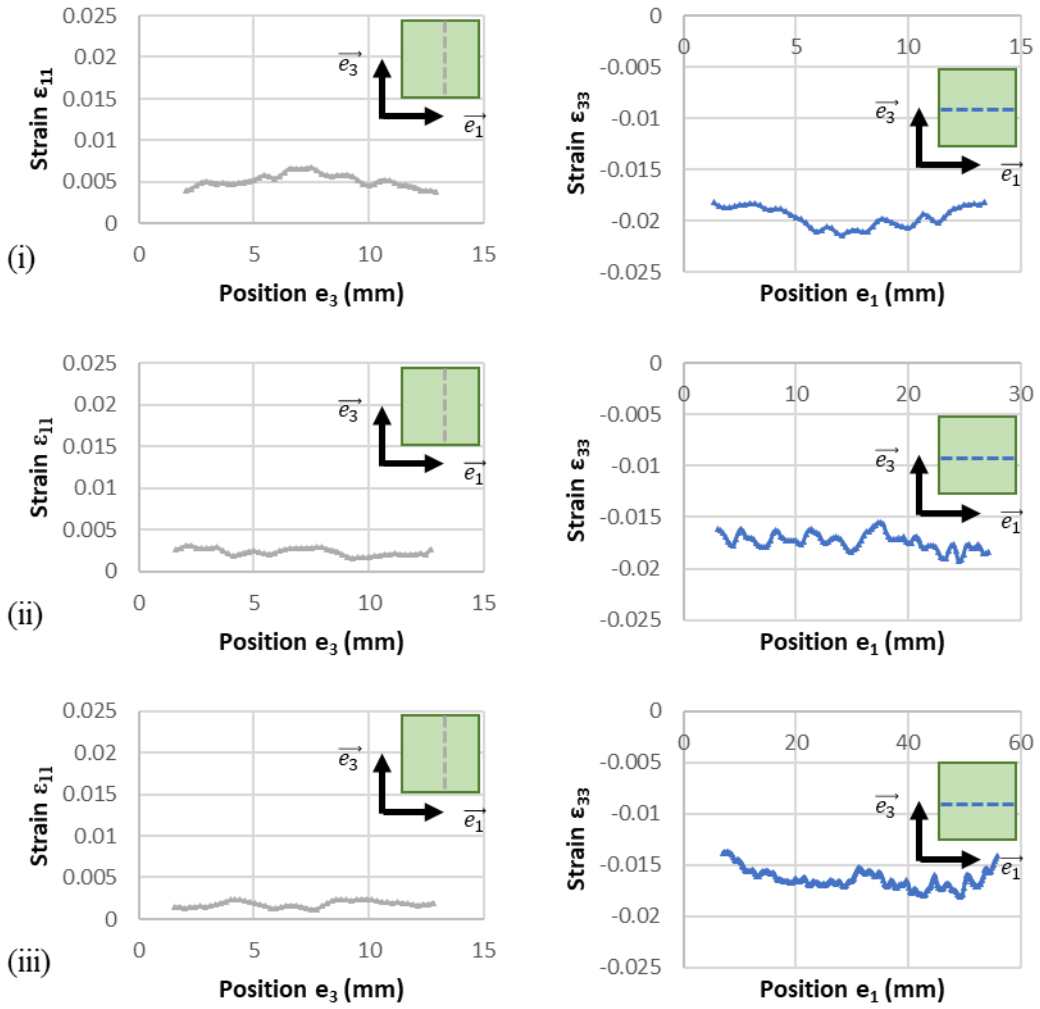

Figure 6: Strain profiles obtained by the "local approach" - (i) set a, (ii), set b, (iii) set c.

Table 2: Experimental results - Stiffness apparent modulus $\boldsymbol{E_3^*}$.

	Apparent elastic modulus E_3^* [MPa]		
	a- 15x15x15 mm^3	b- 30x30x15 mm^3	c- 60x60x15 mm^3
PVC	76.5	79.02	92.6
Standard deviation	2.81	4.68	3.08
rPET	40.6	45.6	53.6
Standard deviation	6.03	9.05	6.79

These apparent parameters will be used to initialize the identification procedure of the parameters by the FEMU method. Accordingly, compression tests were conducted along the $\overrightarrow{e_3}$ axis direction (in the thickness) and along the $\overrightarrow{e_2}$ axis direction on the cubic specimens (a-15x15x15 mm^3). These compression tests resulted in obtaining, in both directions, the

apparent elastic modulus, which corresponds to the slope of the linear part of the stress-strain curve in the longitudinal direction. In contrast, the apparent transverse contraction coefficient (ν_{21}^* or ν_{23}^*) is, in absolute value, the ratio of the transverse strain measured in the direction perpendicular to the axis of solicitation on the longitudinal strain. Figure 7 shows an example of the longitudinal and transversal stress-strain curves of the compression test along the $\overrightarrow{e_3}$ axis direction.

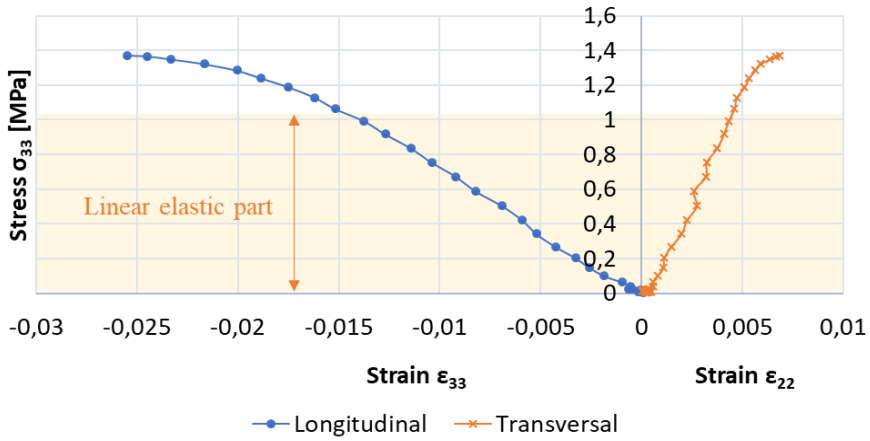

Figure 7: Stress-strain curves (calculation by the "global approach") of compression test in $\overrightarrow{e_3}$ axis direction on PVC specimen (set a-15x15x15 mm^3).

Table 3 represents the different experimental apparent results obtained from the compression tests conducted following longitudinal and transversal directions on the set -a- of specimens.

Table 3: Experimental elastic apparent properties of PVC and rPET foams (15x15x15 mm^3).

	E_2^* [MPa]	E_3^* [MPa]	ν_{21}^*	ν_{23}^*
PVC	50.1	76.5	0.35	0.19
Standard deviation	5.22	2.81	0.02	0.04
rPET	19.7	40.6	0.35	0.15
Standard deviation	5.9	6.03	0.07	0.07

Following the compression tests conducted by subjecting the sample to longitudinal and transversal loading, the stress-strain curves obtained from the two adjacent faces (F1 and F2, as in Figure 3) of the specimen were plotted and compared, as shown in Figure 8. It was found that the transversal strain curves ε_{11} and ε_{22}, for both foams PVC and rPET, were

almost superimposed, indicating that it can be considered an identical strain behavior whatever the transverse direction. This observation is consistent with the assumption of transverse isotropy where ($\overrightarrow{e_1}$, $\overrightarrow{e_2}$) represents the transverse isotropy plane.

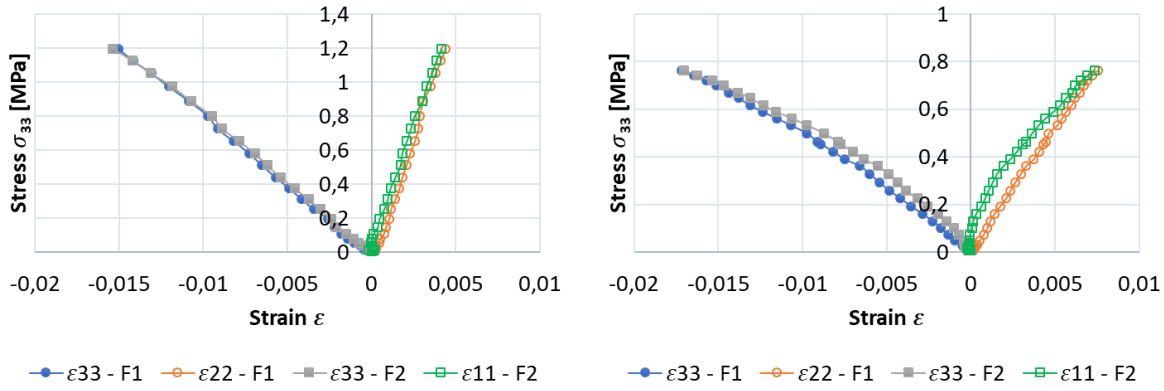

Figure 8: Stress-strain curves for triaxial compression test along $\overrightarrow{e_3}$ axis - PVC and rPET, respectively.

After this observation, a morphological study of the two types of foams was conducted. Several morphological parameters were measured using both SEM and X-ray tomography techniques, such as the average pore area, the average circularity of pores, the pore count per area, and the ligament thickness. For instance, X-ray tomography was carried out on specimens of 6x6x6 mm^3 with a resolution of 3.89 μm for a total of 1390 obtained slices. The acceleration voltage and beam current of the X-ray tube were 50 kV and 115 µA, respectively. It is worth noting that all the obtained slices are normal to the $\overrightarrow{e_3}$ direction. To obtain slices normal to the $\overrightarrow{e_1}$ and $\overrightarrow{e_2}$ directions, a reconstruction of the model using the ImageJ software was performed, followed by cross-sectional sections normal to the $\overrightarrow{e_1}$ and $\overrightarrow{e_2}$ directions. The average pore area was presented in the Materials and methods section of this article in Figure 2 to justify the choice of specimens' dimensions. In contrast, the other parameters are displayed in Figures 9 (i), (ii), and (iii) below. Following these morphological results, each parameter has an equal value in both normal directions, $\overrightarrow{e_1}$ and $\overrightarrow{e_2}$, which differs from the value observed in the $\overrightarrow{e_3}$ normal direction for both foams. Accordingly, this

indicates that the two faces following normal directions, $\overrightarrow{e_1}$ and $\overrightarrow{e_2}$, are morphologically identical. Therefore, these results confirm the previous result that both foams, PVC and rPET, have a transverse isotropic morphology along the $\overrightarrow{e_3}$ normal direction. Consequently, the experimental compression tests and the morphological study results provide evidence for the validity of the transverse isotropy (along the $\overrightarrow{e_3}$ axis) hypothesis in the tested foams herein.

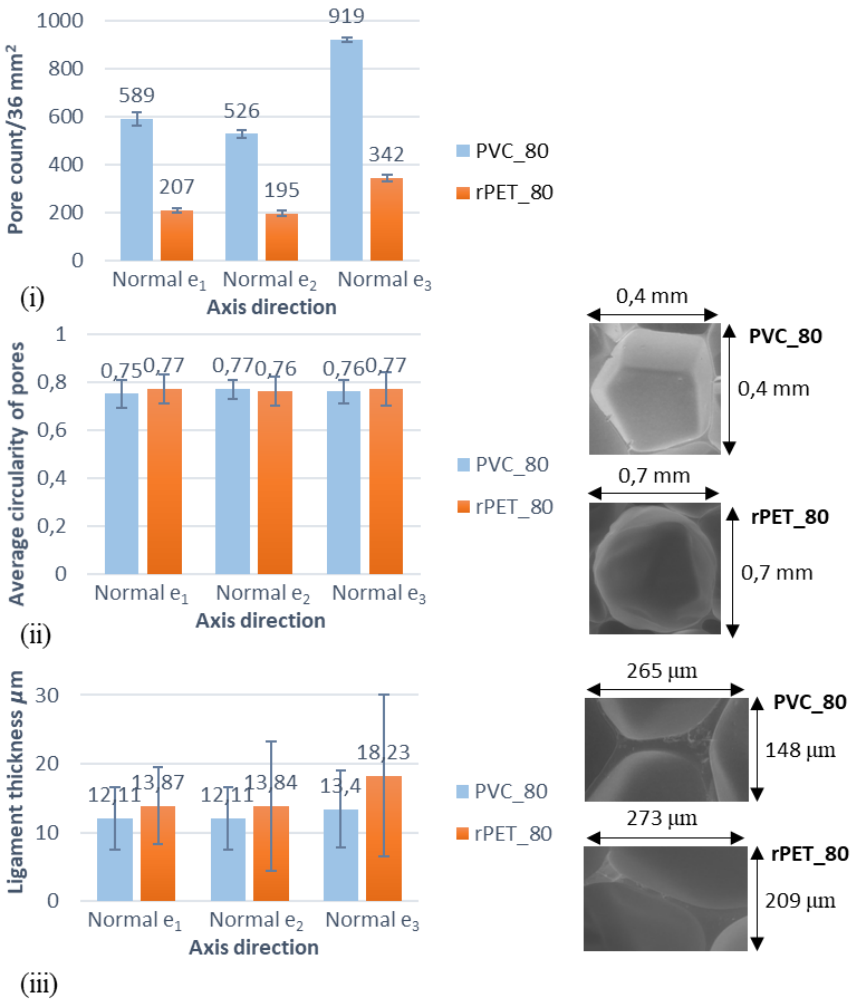

Figure 9: X-ray tomography and SEM results - (i) Pore count/36 mm^2 (ii) Average circularity of pores (iii) Ligament thickness for PVC and rPET foams.

3.3. Uniaxial compression tests

As previously discussed, the specimens can be cut along the $\overrightarrow{e_2}$ or $\overrightarrow{e_1}$ axis direction, allowing a uniaxial compression test to be performed. Since transverse isotropy along the $\overrightarrow{e_3}$ axis has been validated, a uniaxial compression test along the $\overrightarrow{e_1}$ and $\overrightarrow{e_2}$ directions theoretically yields

identical results. Accordingly, specimens of 15x40x15 mm^3 were cut to perform uniaxial compression tests along the $\overrightarrow{e_2}$ axis direction (Figure 3 (ii)). It can be considered that the parameters obtained from these tests are intrinsic since the specimen is in a state of uniaxial stress, and therefore, there is no need to perform the FEMU method in this case. However, these parameters will be used to verify and validate the finite element model used to adjust the other elastic parameters. Table 4 represents the intrinsic elastic parameters measured.

Table 4: Experimental intrinsic results of uniaxial compression along $\overrightarrow{e_2}$ - axis.

	F1		F2	
	E_2 [MPa]	ν_{23}	E_2 [MPa]	ν_{21}
PVC	48.5	0.18	46.7	0.36
Standard deviation	3.5	0.03	2.2	0.03
rPET	18.9	0.16	15.1	0.21
Standard deviation	4.2	0.02	3.8	0.05

3.4. Shear tests

Shear tests in the ($\overrightarrow{e_1}$, $\overrightarrow{e_3}$) plane were conducted on the two foams to identify the shear modulus G_{13}. Using the DIC technique (22), G_{13} was calculated for four observed faces (F1, F2 F3 and F4), resulting in an average value of about 24 MPa with a standard deviation of 1.6 MPa. This modulus is calculated using the formula (1), corresponding to half the slope of the linear part of the stress-strain curve in shear, in which τ_{13} and ε_{13} represent the shear stress and strain, respectively.

$$G_{13} = \frac{\tau_{13}}{2\varepsilon_{13}} \quad (1)$$

The shear tests carried out in this plane identified G_{13} as an intrinsic elastic parameter, as the strain evolution profile, shown on the graph in Figure 10, is constant all over the specimen. Therefore, the use of the FEMU method to adjust the shear modulus for this test is not needed.

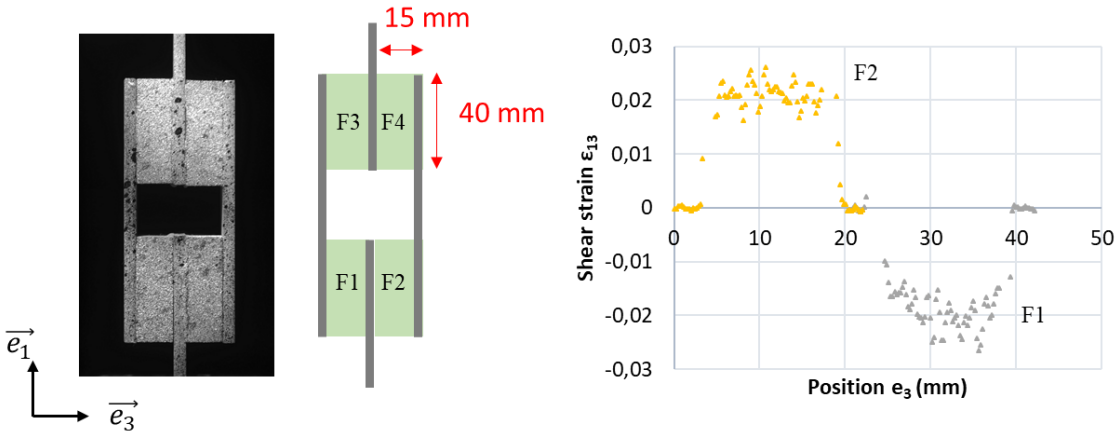

Figure 10: Shear specimen and strain profile ($\overrightarrow{e_1}$, $\overrightarrow{e_3}$).

Since this shear test allowed determining an intrinsic property, other shear tests were also conducted but in the ($\overrightarrow{e_1}$, $\overrightarrow{e_2}$) plane, being the transverse isotropy plane. Once the intrinsic value of the shear modulus G_{12} is determined, the Poisson's ratio ν_{12} can be calculated knowing that $E_1 = E_2$, as the ($\overrightarrow{e_1}$, $\overrightarrow{e_2}$) is the transverse isotropy plane, and using the formula as follows:

$$G_{12} = \frac{E_1}{2(1+\upsilon_{12})} \Rightarrow \nu_{12} = \frac{E_1}{2G_{12}} - 1 \qquad (2)$$

The shear moduli G_{13} and G_{12} are shown in Table 5, as well as the Poisson's ratio ν_{12}.

Table 5: Experimental intrinsic results of shear tests in ($\overrightarrow{e_1}$, $\overrightarrow{e_3}$) and ($\overrightarrow{e_1}$, $\overrightarrow{e_2}$) planes.

	G_{13} [MPa]	G_{12} [MPa]	ν_{12}
PVC	27	17.3	0.39
Standard deviation	2.3	0.2	-
rPET	12.2	8.02	0.18
Standard deviation	1.7	1.04	-

For the two foams, the Poisson's ratios ν_{12} resulting from shear tests (Table 5) and ν_{21} resulting from uniaxial compression tests along the $\overrightarrow{e_2}$ axis direction (table 4) are equivalent.

4. Numerical elastic model

As mentioned earlier, based on the literature, PVC foams are transversely isotropic. Accordingly, using this hypothesis, the compliance matrix S of an elastic transversely

isotropic material is given in the matrix form as written in the following linear elasticity relation:

$$\varepsilon_{ij} = S_{ijkl}\,\sigma_{kl} \tag{3}$$

The equation 4 below is obtained using Voigt notation:

$$\begin{pmatrix} \varepsilon_{11} \\ \varepsilon_{22} \\ \varepsilon_{33} \\ 2\varepsilon_{12} \\ 2\varepsilon_{13} \\ 2\varepsilon_{23} \end{pmatrix} = \begin{bmatrix} \frac{1}{E_1} & \frac{-\nu_{21}}{E_2} & \frac{-\nu_{31}}{E_3} & 0 & 0 & 0 \\ \frac{-\nu_{12}}{E_1} & \frac{1}{E_2} & \frac{-\nu_{32}}{E_3} & 0 & 0 & 0 \\ \frac{-\nu_{13}}{E_1} & \frac{-\nu_{23}}{E_2} & \frac{1}{E_3} & 0 & 0 & 0 \\ 0 & 0 & 0 & \frac{1}{G_{12}} & 0 & 0 \\ 0 & 0 & 0 & 0 & \frac{1}{G_{13}} & 0 \\ 0 & 0 & 0 & 0 & 0 & \frac{1}{G_{23}} \end{bmatrix} \begin{pmatrix} \sigma_{11} \\ \sigma_{22} \\ \sigma_{33} \\ \sigma_{12} \\ \sigma_{13} \\ \sigma_{23} \end{pmatrix} \tag{4}$$

The notations 1, 2, and 3 correspond respectively to the $\overrightarrow{e_1}$, $\overrightarrow{e_2}$, and $\overrightarrow{e_3}$ axes. Knowing that for a transversely isotropic material where ($\overrightarrow{e_1}$, $\overrightarrow{e_2}$) is the isotropy plane: $E_1 = E_2$; $\nu_{12} = \nu_{21}$; $\nu_{13} = \nu_{23}$; $\nu_{31} = \nu_{32}$; $G_{13} = G_{23}$. The determination of the compliance matrix S is done by determining five elastic coefficients, E_1 or E_2, E_3, ν_{12}, ν_{13}, and G_{13}. Based on this transversely isotropic hypothesis and given that the experiments determined four intrinsic elastic parameters, E_2, ν_{12}, ν_{23}, and G_{13}, the remaining elastic parameter is E_3. The latter cannot be determined experimentally due to the limitations of the uniaxial compression theory, as previously explained in this paper. Therefore, a finite element model updating method was employed to determine this parameter by defining the material as a transversely isotropic where ($\overrightarrow{e_1}$, $\overrightarrow{e_2}$) is the isotropy plane.

4.1. Model dimensions and boundary conditions

A numerical method has been implemented to identify the intrinsic elastic parameters, experimentally established but considered apparent rather than intrinsic. A finite element model, as shown in Figure 11, was created on Abaqus, where two symmetries about ($\overrightarrow{e_1}$, $\overrightarrow{e_3}$)

and ($\overrightarrow{e_2}$, $\overrightarrow{e_3}$) were applied. Displacements were applied to the boundaries according to the experiments. In other words, the imposed boundary conditions correspond to a state of triaxial compression, allowing the description of the compression tests carried out. The displacement along the $\overrightarrow{e_3}$ axis on the top face of the sample generates the compressive force, whereas, on the bottom face, the displacement along the $\overrightarrow{e_3}$ axis is blocked. On the other hand, a displacement on each of the two lateral faces was imposed to ensure a stress state identical to that obtained by performing the experimental test. These displacements are found following the calculation of the transverse strains by the image correlation method. The displacement $U(t)$ applied on the face of normal $\overrightarrow{e_1}$, $\overrightarrow{e_2}$, and $\overrightarrow{e_3}$ was calculated from the global strain $\varepsilon_{11}(t)$, $\varepsilon_{22}(t)$, and $\varepsilon_{33}(t)$, respectively, and the width L of the sample in this direction. Accordingly, these displacements are calculated as follows:

$$U_{e_1}(t) = \varepsilon_{11}(t) . \frac{L_{e_1}}{2} \quad (5); \qquad U_{e_2}(t) = \varepsilon_{22}(t) . \frac{L_{e_2}}{2} \quad (6); \qquad U_{e_3}(t) = \varepsilon_{33}(t) . L_{e_3} \quad (7)$$

Furthermore, this model has been linked to Matlab through Python to manage its input parameters easily. It will be explained in detail in the following section.

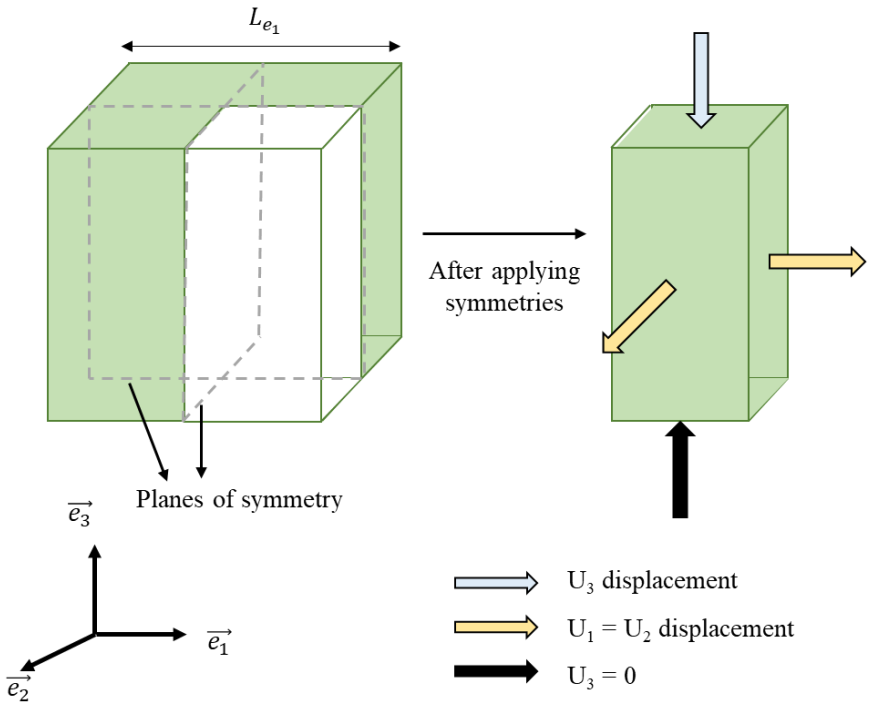

Figure 11: FE model and boundary conditions.

4.2. Optimization loop

To organize the recalibration method, an interface on Matlab was created. It was linked to the Python code by defining the input parameters in this interface (specimen's dimensions, mesh size, material properties, etc.). Moreover, a loop was also created in which the error between the experimental results and the numerical ones is calculated. This error is minimized after implementing it with the suitable other parameters in the minimizing function in Matlab. Once the minimal residual value is reached, the loop stops, and the intrinsic elastic parameters are obtained. These optimized parameters correspond to the minimal error possible. Although certain parameters have been identified intrinsically through experiments, they are also identified using this FEMU method. This identification enables the comparison between the values obtained both numerically and experimentally. This method is a generalized approach for performing a finite element model updating method (FEMU) based on minimizing the error between the experimentally obtained results and numerical results for each set of input parameters. In this article, the materials under consideration are PVC and rPET foams. Since both foams present a homogeneous strain field, as shown in Figures 6 (i), (ii), and (iii), the FEMU method was used with a fixed single-element mesh parameter.

4.3. Numerical calculations

A sensitivity matrix for the adjusted elastic parameters was calculated. It was found that Young's moduli E_2 and E_3 are the influential parameters, as opposed to Poisson's coefficients ν_{23} and ν_{21}. The results of the sensibility matrix are shown in Table 6.

Table 6: Sensibility matrix for δ = 5%.

	E_2	ν_{23}	E_3	ν_{21}
Sensibility [%]	22.4	0.13	69.5	0.01

The different compression tests along the longitudinal direction for the three sets of specimen dimensions (a, b, and c) and along the transverse direction were modeled to adjust the different elastic parameters. This adjustment requires calculating an average total error in force of these four tests simulated in parallel. As mentioned earlier, these numerical tests are conducted using displacement boundary conditions established from measured strain fields, and the average total error in force is thus the average of the force errors of the different compression tests in both directions. These force errors are calculated by summing the errors across all time points, where at each point on the curve, the numerical value is compared to the experimental value, and the resulting error is squared. The sum of all these squared errors yields the total error for each set of specimen dimensions. The error resulting from the compression test in the transverse direction was assigned a weight of 3, as only one set of specimen dimensions was tested in this direction, and the sensibility value of the E_2 modulus is about one-third of E_3. Consequently, the average total error is calculated using the formula (8).

$$Err\ average\ =\ \frac{(err_{L-a}\ +\ err_{L-b}\ +\ err_{L-c}\ +\ \mathbf{3}\ *\ err_T)}{6} \qquad (8)$$

Whereas $Err\ average$ represents the average total error, err_{L-a}, err_{L-b}, and err_{L-c} correspond to the squared errors resulting from the longitudinal compression test on the sets of specimen dimensions a, b, and c, respectively. Moreover, err_T is the squared error resulting from the compression test in the transverse direction. The adjusted parameters are displayed in Table 7, while an example of the total error evolution and the stress-strain curves are shown on graphs (i) and (ii), respectively, of Figure 12.

Table 7: Numerical optimized elastic parameters.

	E_2 [MPa]	ν_{23}	E_3 [MPa]	ν_{21}
PVC	48.1	0.18	74.4	0.36
rPET	19.1	0.15	42.9	0.32

5. Analysis and discussions

Based on the graph (ii) of Figure 12, the green curve with the triangle pattern is drawn numerically using the apparent parameters found experimentally as input properties, while the blue curve with the dash pattern is drawn directly using the experimental values. On the other hand, the red curve with the square pattern is the one plotted using the adjusted parameters. The values in Table 7 correspond to the red curve in Figure 12.

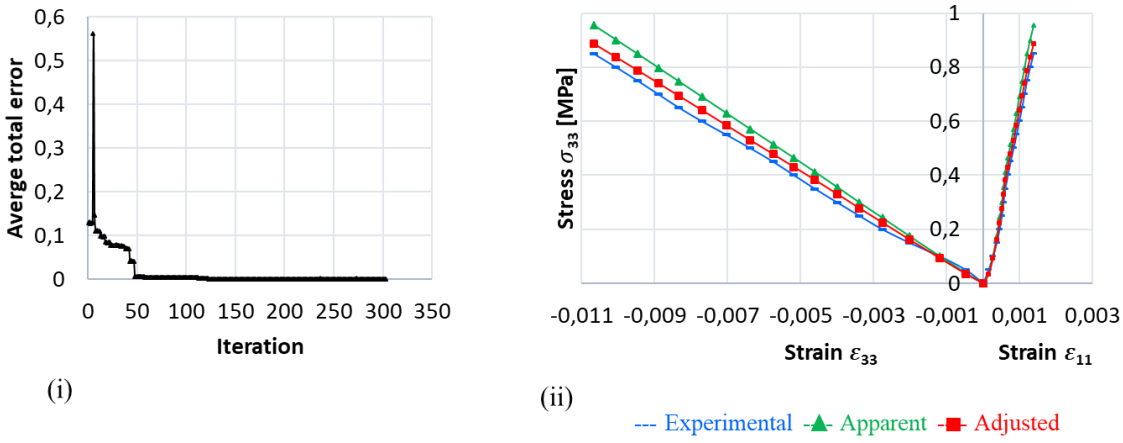

Figure 12: (i) Total error evolution, (ii) Stress-strain evolution for the set b of PVC specimens.

Since Poisson's coefficients were not found influential, their values displayed in Table 7 are not representative. This result is due to the fact that the FEMU method herein was realized based on adjusting force values. For instance, when this FEMU is performed based on displacement values, the Poisson's coefficients become influential, and their numerical values will therefore be representative (20). But these two coefficients were already calculated, and their values were found intrinsic, as explained in the Triaxial compression tests and Uniaxial compression tests sections, as well as Young's Modulus E_2. The latter validates the reliability of this adjusting method by comparing its intrinsic experimental value to the numerical adjusted one obtained. Experimentally, E_2 has a value of about 48.5 MPa with a standard deviation of 3.5 MPa and about 46.7 MPa with a standard deviation of 2.2 MPa for the faces

F1 and F2, respectively, of the PVC specimens (Table 4). By comparing the numerical adjusted value of 48.1 MPa to the ones obtained experimentally and considering the standard deviation, E_2 obtained from both methods is found equal. By doing the same for the rPET foam, both the numerically and experimentally obtained E_2 are identical. This result allowed the validation and verification of the FEMU used herein. Hence, the value of Young's modulus E_3 is intrinsic and is equal to 74.4 MPa and 42.9 MPa for the PVC and rPET foams, respectively, while both are smaller than the values measured experimentally for the three sets of specimens' dimensions (a-b-c). This finding is logical and acceptable as the experimental properties are apparent. Thus, the experimental measurements are often subject to uncertainties and errors, leading to overestimation in the calculation of the material parameters. As such, the FEMU method tries to minimize the impact of such issues on the calibration process, resulting in smaller and more accurate adjusted values. On the other hand, the FEMU method relies on adjusting the parameters until the predicted response of the model matches the experimental measurements, assuming the model accurately represents the material's behavior. However, as the model may not be able to capture all the physical properties, the FEMU method results in smaller values of the parameters. Upon examination of the datasheets and the adjusted parameters, it was observed that the E_3 values in the datasheets are consistently higher than the adjusted values for both foams. These observations were consistent with the suggestions mentioned above that the standardized tests seem to precisely assume that the sample is in a uniaxial state of stress and thus calculate the various elastic parameters using the formulas of a uniaxial compression test. Since, in this study herein, the compression is not uniaxial, the consequent datasheet values obtained from these standardized tests contribute to an overestimation of the parameters.

6. Conclusions

This study identified the intrinsic elastic behavior of two polymer foams used as core materials for sandwich structures. This research was conducted based on an original method combining several experimental or numerical approaches. Digital image correlation (DIC) technique was applied to determine the different strain values of each specimen for the different tests carried out. Accordingly, the experimental part led to determining some intrinsic parameters of the foam. Nevertheless, some parameters obtained are considered apparent due to the multiaxial state of stress found experimentally. These apparent properties, as well as morphological parameters, were used to validate the transverse isotropy behavior of the two foams PVC and rPET. After confirming this hypothesis, the study was completed by a FE model on Abaqus linked to a minimization function on Matlab, which resulted in identifying the intrinsic values of the other parameters. Moreover, the reliability of this method was tested by comparing one of its resulting parameters to the corresponding one from the uniaxial compression test conducted experimentally. A good correlation was found between numerical calculations and experimental results. This study will be complemented with a plastic characterization to establish the overall homogenized behavior of the foam.

Acknowledgment

The authors would like to acknowledge the support provided by the Occitanie region in France and the WINDELO company for this project.

References

1. Testouri A. Highly structured polymer foams from liquid foam templates using millifluidic lab-on-a-chip techniques. PhD Thesis, Université Paris Sud XI; 2012.
2. Pérez-Tamarit S, Solórzano E, Hilger A, Manke I, Rodríguez-Pérez MA. Multi-scale tomographic analysis of polymeric foams: A detailed study of the cellular structure. *Eur Polym J*. 2018;109:169–178.
3. Dabo M, Roland T, Dalongeville G, Gauthier C, Kékicheff P. Ad-hoc modeling of closed-cell foam microstructures for structure-properties relationships. *Eur J Mech A/Solids*. 2019;75:128–141.

4. Pehlivan L, Baykasoğlu C. An experimental study on the compressive response of CFRP honeycombs with various cell configurations. *Compos Part B Eng*. 2019;162:653–661.
5. Carranza I, Crocombe AD, Mohagheghian I, Smith PA, Sordon A, Meeks G, et al. Characterising and modelling the mechanical behaviour of polymeric foams under complex loading. *J Mater Sci*. 2019;54(16):11328–11344.
6. Gupta N, Ye R, Porfiri M. Comparison of tensile and compressive characteristics of vinyl ester/glass microballoon syntactic foams. *Compos Part B Eng*. 2010;41(3):236–245.
7. Rizov VI. Elastic–plastic response of structural foams subjected to localized static loads. *Mater Des*. 2006;27(10):947–954.
8. Youssef S, Maire E, Gaertner R. Finite element modelling of the actual structure of cellular materials determined by X-ray tomography. *Acta Mater.* 2004;53(3):719–730.
9. Francisco M, Júnior C, Soares GP, Angélico RA, Canto RB, Tita V. Study of an Anisotropic Polymeric Cellular Material Under Compression Loading. *Mater Res.* 2012;15(3):359–364.
10. Luong DD, Pinisetty D, Gupta N. Compressive properties of closed-cell polyvinyl chloride foams at low and high strain rates: Experimental investigation and critical review of state of the art. *Compos Part B Eng.* 2013;44(1):403–416.
11. Viana GM, Carlsson LA. Mechanical Properties and Fracture Characterization of Cross-Linked PVC Foams: *J Sandw Struct Mater.* 2002;4(2):99–113.
12. Tita V, Caliri MF, Angélico RA, Canto RB. Experimental analyses of the poly(vinyl chloride) foams' mechanical anisotropic behavior. *Polym Eng Sci*. 2012;52(12):2654–2663.
13. Espadas-Escalante JJ, Avilés F. Anisotropic compressive properties of multiwall carbon nanotube/polyurethane foams. *Mech Mater.* 2015;91(P1):167–176.
14. Hamilton AR, Thomsen OT, Madaleno LAO, Jensen LR, Rauhe JCM, Pyrz R. Evaluation of the anisotropic mechanical properties of reinforced polyurethane foams. *Compos Sci Technol.* 2013;87:210–217.
15. Juntikka R, Hallstrom S. Shear characterization of sandwich core materials using four-point bending. *J Sandw Struct Mater.* 2007;9(1):67–94.
16. Yonezu A, Hirayama K, Kishida H, Chen X. Characterization of the compressive deformation behavior with strain rate effect of low-density polymeric foams. *Polym Test.* 2016;50:1–8.

17. Ustinova OV. The crush behaviour of Rohacell-51WF structural foam. Int J Solids Struct. 2000;37(43):6321–6341.
18. Tita V, Caliri MF. Numerical simulation of anisotropic polymeric foams. *Lat Am J Solids Struct.* 2012;9(2):259–279.
19. Bilkhu SS, Founas M, Nusholtz GS. Material Modeling of Structural Foams in Finite Element Analysis Using Compressive Uniaxial and Triaxial Data. *SAE Tech Pap 930434*. 1993;21.
20. Ienny P, Caro-Bretelle A-S, Pagnacco E. Identification from measurements of mechanical fields by finite element model updating strategies. *Eur J Comput Mech.* 2009;18(3–4):353–376.
21. Giton M, Caro-Bretelle AS, Ienny P. Hyperelastic behaviour identification by a forward problem resolution: Application to a tear test of a silicone-rubber. *Strain.* 2006;42(4):291–297.
22. Caro-Bretelle AS, Ienny P, Nait-Ali LK, Bergeret A. Dissipative behaviour analysis of reprocessed polyethylene terephthalate using digital image correlation and updated finite element analysis. *Strain.* 2013;49(2):135–146.
23. DIN EN ISO 844:2021. Rigid cellular plastics – Determination of compression properties.
24. Astm International 2020. Astm c393/c393m-20 Standard Test Method for Core Shear Properties of Sandwich Constructions by Beam Flexure.
25. ISO 1922:2018. Rigid cellular plastics – Determination of shear properties.